Charge spreading from a point source in a depleted diode

R F Fowler, J V Ashby and C Greenough

September 1998

Abstract

This report describes simulations that have been made of the charge spreading that occurs in a semiconductor from a point generation event such as an X-ray strike. Simulations have been made using two- and three-dimensional blocks of silicon which are biased so as to produce very large depletion regions. Any charge generated in these regions will be transported to collecting contacts. The device modelling software package EVEREST has been modified to allow measurement of the charge spreading that occurs from the impact up to the time the charge is collected at a contact. Numerical results are compared to a simple diffusion model for 2D and 3D cases. The model is in reasonable agreement with the results at low charge density in 2D. Larger differences between the 3D measurements and the theory may be due to limitations of the simulation mesh size. A functional form for the spreading from any depth and reasonable size of charge event can be derived which may be used in analysis of CCD and pixel detector performance.

A copy of this report can be found at the Department's web site (*http://www.dci.clrc.ac.uk/*) under page *Group.asp?DCICSEMSW* or anonymous ftp server *www.inf.rl.ac.uk* under the directory *pub/mathsoft/publications*

Mathematical Software Group
Department for Computation and Information
Rutherford Appleton Laboratory
Chilton, DIDCOT
Oxfordshire OX11 0QX

Contents

1 Introduction

In this report we give some results of charge spreading obtained using the EVEREST device modelling software package [3]. This package has recently been enhanced to include charge generation events, such as those caused by X-ray strikes on a silicon detector. The main details of these changes are described in [2]. Some further updates to the software that have been made explicitly to help in measurement of charge spreading are described in this report.

We investigate the spreading of the charge by the time it is collected at the contact as a function of the depth of the event and the energy involved (i.e. the number of electron-hole pairs generated). The lateral spread of a charge packet from the point at which it is generated up to the time it is collected, either under a CCD gate or by the appropriate read out contact in a pixel detector, is important in determining the sensitivity of the device. Ideally all the charge generated by a single event would be collected by one contact, but this is not always the case, since events can occur close to the edge of one contact with the next. Then the charge will be split between two of more contacts which will make correct interpretation of the data more difficult. The charge spreading data enables one to determine the size of the regions in which the event is not uniquely detected by a single contact.

Modelling of the operation of X-ray analysis equipment, and the associated detectors, is important to allow optimisation of the design. Within the IMPACT [7] project use has been made of the software package MCNP [1] to calculate the expected distribution of X-ray strikes within a given detector design. Given this information it is then desirable to know what response will then be produced by the semiconductor detector. One way to do this would be to use EVEREST to simulate the results from each possible charge generation event and then to average the outputs appropriately. However, due to the long simulation times required, this would be prohibitively expensive. Instead it is more realistic to characterise aspects of charge transport within a detector using EVEREST to simulate a selected number of cases and them finding a suitable functional form to interpolate this data over all cases of interest.

As an example, the MCNP program may be used to predict the distribution function for the location and energy of events generated within a silicon detector. It would then be useful to predict what proportion of these events are successfully registered by a single pixel of the detector. This can be done if information is available on how the charge generated at any given point spreads out as it is transported to the collecting contacts.

In this report a simple analysis is made of the expected spreading of charge based on a diffusion model. This is then compared with simulation results from EVEREST in both two and three dimensions. The difference between the basic analysis and the simulation results is an indication of the importance of charge self interaction. Combining the measured charge spreading results with the functional form found by approximate analysis gives a simple expression for charge spreading which can be used in combination with results from MCNP.

2 Test structures

Simulations of charge spreading have been made in 2D and 3D devices using EVEREST. The structures used are simple p-n diodes of rectangular geometry, as shown in Figure 1.

Figure 1: *Geometry of the 2D diode structure. The n-type region is lightly doped while the small p-type region is heavily doped. For 2D simulations in EVEREST the device size is* $100 \times 40 \times 1\mu m$. *For the 3D simulations the size is* $100 \times 50 \times 50$.

The commands to generate the 2D structure in the EVEREST pre-processor are listed below. For a full description of the EVEREST modules and commands see the user manuals [4].

```
BLOCKS
NEUT P-NW
VOL V11 B ( 0  0  0) (  2 20 1) SILICON
VOL V12 B ( 0 20  0) (  2 20 1) SILICON
VOL V21 B ( 2  0  0) ( 98 20 1) SILICON
VOL V22 B ( 2 20  0) ( 98 20 1) SILICON
CON CP R (  0  0 0,   0 40 0,   0 0 1)
CON CN R (100  0 0, 100 40 0, 100 0 1)
GEN
END
MESH
NEUT P-NW
REF L009 20 0
REF L033 20 0
REF L004 20 0
REF L016 20 0
END
END
```

The given mesh commands generate a uniform grid of 3362 nodes and 1600 hexahedral elements. A similar device but with 3D meshing is given by the commands file:

```
BLO
NEU PN3D
VOL V1 BRICK (0 0 -100) (50, 50, 98) SI
VOL V2 BRICK (0 0   -2) (50, 50,  2) SI
CON CP R (0 0    0, 0 50    0, 50  0    0)
CON CN R (0 0 -100, 0 50 -100, 50  0 -100)
GEN
END
MESH
NEUT PN3D
REF L013  5 0
REF L001 38 0
REF L014 20 0
REF L022 20 0
END
END
```

In this case the mesh used has 19404 nodes and 17200 elements. Note that a different orientation has been used from the 2D case. In fact the 3D problems analysed in this work have cylindrical symmetry, so they could be treated more efficiently if this symmetry was recognised by the solver. EVEREST does not have this capability at present, so a full 3D mesh must be used.

The devices are lightly doped in the large $98\mu m$ long n-region ($3\times10^{12}cm^{-3}$) while a small p-region of $2\mu m$ is doped at $1\times10^{17}cm^{-3}$. The n-region is fully depleted with a reverse bias of $40V$. A few simulations have also been made on a $300\mu m$ structure in 2D. In this case the n-region has just been extended to $298\mu m$ while the doping has been kept constant. To fully deplete this longer device requires in excess of 200V at this doping level.

Note that to measure the spread of charge at a contact it is important that the device is fully depleted right up to that contact. Even a very small non-depleted region in front of the contact will allow the charge to be distributed almost uniformly across all contact nodes. Strictly speaking a contact to a lightly doped region will not behave as a pure ohmic contact, but this is not important for these simulations of charge spreading. EVEREST treats all semiconductor contacts as ohmic.

In all test cases a charge generation event at time $t = 0$ is introduced at a depth d on the centre line of the device. For 2D simulations two events are used one at $z = 0$ and one at $z = 1$, so as to ensure symmetry in the third direction. For 3D simulations, a single event is used on the centre line.

3 Measuring charge spreading at contacts

Initial charge spreading measurements were made in the 2D simulations using up to 20 individual contacts, each of width $1\mu m$ with the same distance between contacts. While this proved feasible in 2D geometries, it is much harder to do in 3D and EVEREST imposes a number of limits on the total number of contacts that can be used.

A more practical approach is to add a new command which will indicate the contact of interest over which the charge integral is required. The `INTEGRATE` command has been added to the latest version of the EVEREST solver for this purpose. This command takes two parameters, the name of the contact of interest and the file in which the results are to be stored. For example,

```
INTEGRATE SOURCE EVER-SOURCE-01
```

would request the integration of current collected at the `SOURCE` contact on a node by node basis with the results stored in the file `EVER-SOURCE-01`. Note that at present it is only possible to perform the integration on one device contact in a simulation. If a second integration command is issued it replaces the first command.

When a contact is selected for integration, the current arriving at each individual node on the contact is integrated over time. This is the current flowing through the control area associated with the node. The results of this integration are written to the output file at each time step specified in the `TIME` command. The file is of ASCII format and contains 5 columns of data. The first three values are the x, y and z coordinates of the contact node. The next two values are the integral of the hole and electron currents that have arrived at that node up to the given time. The displacement current integral is not given, as we are mainly interested in charge spreading. The order of the nodes in the file is not regular so the user will have to sort results to get meaningful charge spreading data. In addition, we only output the raw current integral data. If the mesh is not fully regular on the contact plane it will be necessary to normalise the current integrals by dividing by the control area around each contact node, which must be done by the user. In all simulations to date the mesh on the contact has been regular, and hence normalisation is not needed to extract the charge distribution pattern.

The actual integration method used is very simple and is not quite as accurate as the integration used in the post-processor to get the total charge collected at contacts. Hence the sum of values in the output file will not be identical to the value given by the post-processor. If long simulation times are used it may be necessary to correct nodal charge results for the effects of leakage current. However it is usually easier to select an integration time which is short enough to gather all the generated charge, but not so long as to give a significant leakage current contribution.

To extract an ordered 2D profile of the charge collected along say the line $y = 25$ on the contact it is necessary to sort the results data file. This can be done by hand in an editor or using Unix tools such as *awk* and *sort*.

4 Approximate expression for charge spreading

In these simple test structures the charge is generated as a concentrated cloud at one or two mesh nodes. The holes and electrons then move outwards due to diffusion and apart from each other due to the applied electric field. The field is linear within most of the n-region as shown in Figure 2. We are interested in finding the dependence of the spreading of the charge on the depth at which the generation event occurs.

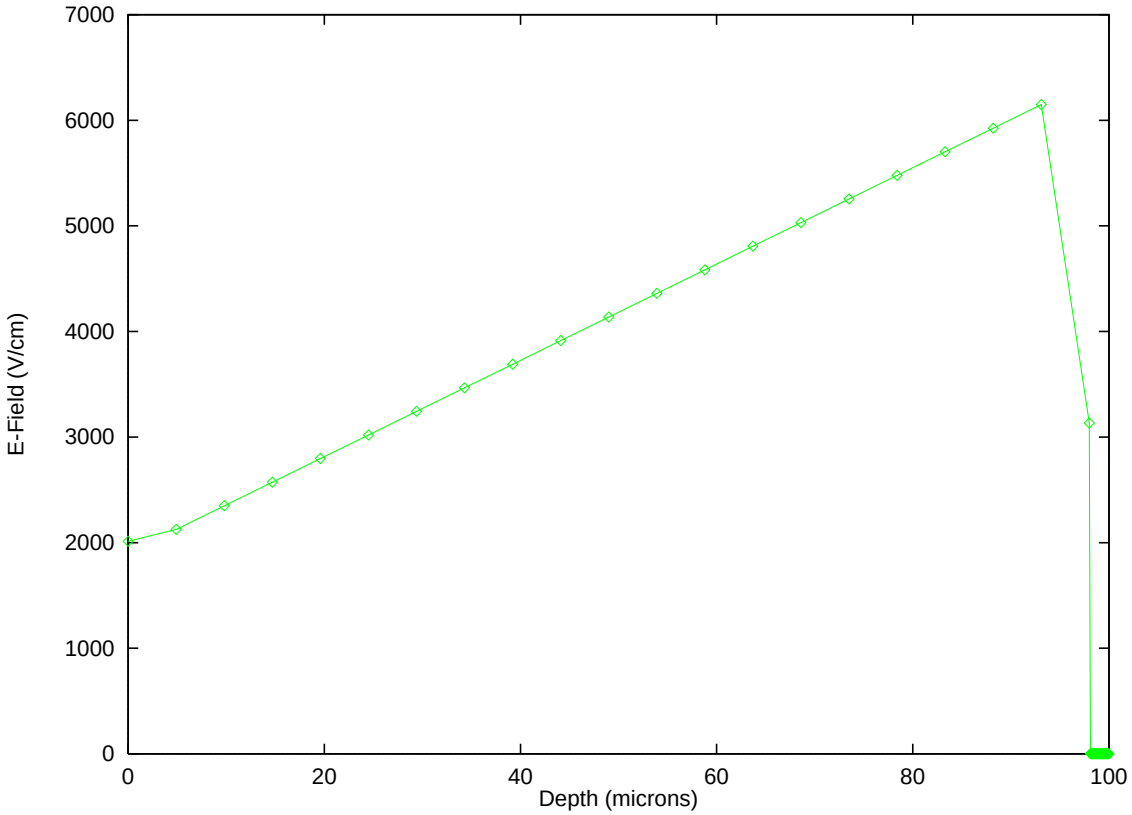

Figure 2: *Electric field in the 40V reverse bias case with full depletion in the n region. This is the solution before the charge generation event occurs.*

To obtain an approximation to the spreading of charge, consider the electron cloud as it moves towards the positive contact. If the diffusion of the charge along the field direction is ignored, then it is possible to calculate an expected transit time T_t for the electrons to reach the contact from an event at depth d. Since the electric field is linear it can be expressed as

$$E(x) = \alpha + \beta x \tag{1}$$

where α and β are positive constants if the n-region runs from $x = 0$ to $x = 98$ and the p-region from $x = 98$ to $x = 100$. The drift velocity of an electron as a function of position x is then

$$v(x) = -\mu E(x) = -\mu(\alpha + \beta x) \tag{2}$$

where μ is the electron mobility, which will be assumed to be constant[1]. The transit time for

[1] The effect of field dependent mobility is discussed in the 2D results section of this report.

an electron to get from depth d to the $x = 0$ contact is given by

$$T_t = \int_d^0 dx \frac{dt}{dx} = \frac{1}{\mu} \int_0^d dx \frac{1}{\alpha + \beta x} \tag{3}$$

$$= \frac{1}{\mu\beta} [\log(\alpha + \beta x)]_0^d \tag{4}$$

$$= \frac{1}{\mu\beta} \log(1 + \frac{\beta}{\alpha} d) \tag{5}$$

In addition to ignoring the effect of diffusion along the direction of the electric field, the above value also ignores the effect of the charge clouds on the field.

If the spreading is now treated as a simple 2D diffusion problem the charge density at the contact will be given by the solution of the diffusion equation for a delta function distribution at time $t = 0$. The standard solution is of the form (see e.g. [6]):

$$n(r, t) = \frac{\gamma}{t} \exp(-\frac{r^2}{2\varepsilon t}) \tag{6}$$

where $\varepsilon = 2D$ and D is the diffusion constant. In this case r is the radial distance from the centre line. Thus the width of the Gaussian is expected to be

$$\sigma_t^2(d) = \varepsilon T_t = 2D \frac{1}{\mu\beta} \log(1 + \frac{\beta}{\alpha} d) \tag{7}$$

The diffusion constant is related to the mobility by $D = \mu kT/q$, so this expression becomes,

$$\sigma_t^2(d) = \varepsilon T_t = \frac{2kT}{q\beta} \log(1 + \frac{\beta}{\alpha} d) \tag{8}$$

In the case of $\beta << \alpha$, when the applied field is very much stronger than that due to fixed charge, the right hand side is proportional to d and hence $\sigma \propto \sqrt{d}$. In other cases, this equation predicts a weaker than square root dependence of σ on d. It also predicts that the hole and electron spreading should be the same, since the mobility term cancels out.

For the electric field in Figure 2 the linear portion of the result is well fitted with $\alpha = 0.1923 V/\mu m$ and $\beta = 4.53 \times 10^{-3} V/\mu m^2$. As long as the voltage is high enough that the n region is fully depleted then the gradient β should remain the same, while α will increase with V.

5 EVEREST solutions

Simulations have been performed on the 2D and 3D P-N structures using a range of charge event sizes at varying depths. While we are mainly interested in the 3D results, the 2D simulations can be performed more quickly and with better resolution due to the finer mesh. In the simple model of charge spreading discussed in the previous section the 3D result would just be the product of two Gaussian distributions with the same width as the 2D result.

A typical run file for a simulation with a charge generation at a depth of $50\mu m$ is shown below. Details of the meaning of these commands can be found in the user manual [4].

```
GEO P-NW
MES P-NW
DOP P-NW
PHY P-NW R
CAT P-NW R
OUT P-NW R
BIAS CN (0.0,-80)
BIAS C1 (0)
MAT SI LMUOP=4.5D2 LMUON=1.5D3
MOD MOB=LAT REC=NONE
SOLVE TYPE=ST START=0 GUMLIM=4 ICCGTOL=1D-10 CGSTOL=1D-10
TIMES (1D-8 2D-8)
CUE POINT (50 20 0) 100 0
CUE POINT (50 20 1) 100 0
INTEGRATE C1 CINT100-50-100V80
SOLVE TYPE=TRA START=2 TRANTOL=1E-4
END
```

The simulations have been carried out to $20ns$, with results output at $10ns$ and $20ns$. This is long enough for all the charge to be collected, but not so long that leakage current becomes a significant contribution. Since the charge is all collected in under $1ns$ it is possible to correct for leakage current by comparing the two different time results, thought the correction in this case is very small. On a SUN SPARC10 a typical 2D simulation takes of the order of 2.5 hours, while the 3D simulations take about 10 hours.

To view the charge distribution within the device as it moves towards the collecting contact, the solution can be written to file at various intermediate times. This generates a large amount of data which is unnecessary for measurement of charge spreading. However, it can be useful to view the shape of the charge cloud, particularly given the approximation used in the previous section that diffusion along the direction of the field can be ignored. In Figure 3 results are shown for the charge density at various times for a simulation on the 3D mesh with 250 electron-hole (e-h) pairs generated at the centre point. In this case results are for the hole density on the $y = 25$ plane and the charge moves to the heavily doped p-region. The contours are plotted on a logarithmic scale which emphasises the actual spread but it is clear that the assumption of a point charge moving in the field is far from the actual situation.

Figure 4 shows a series of results for the measured charge distribution in the 2D device as a function of the depth of the event. A total charge of 200 electron hole pairs has been used in these simulations over the width of $1\mu m$. The charge distribution can be seen to follow a

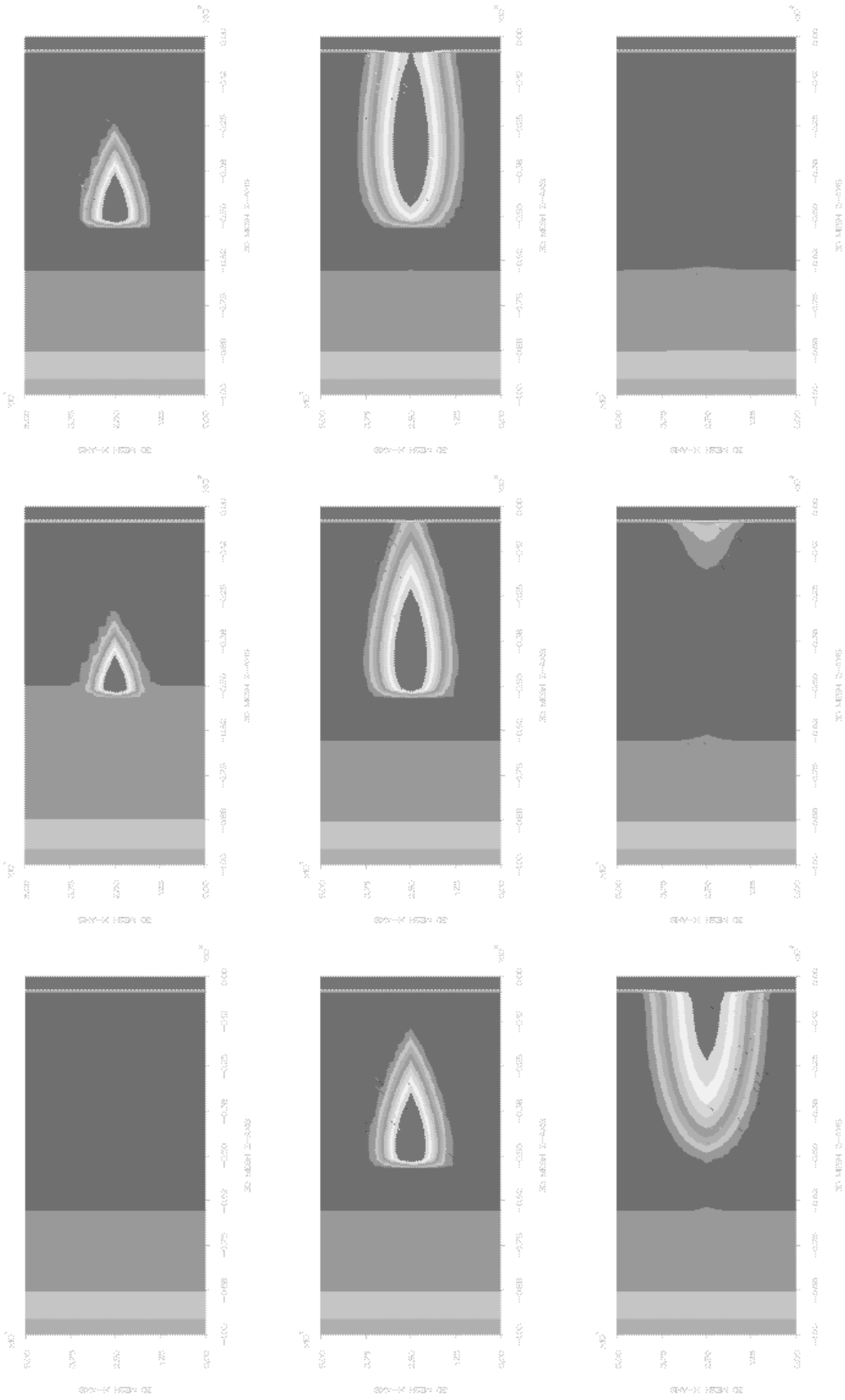

Figure 3: *Charge transport along the centre plane of the 3D device. The lower left picture is the initial state, before impact, of the hole density (log scale). The picture above it is after 8ps, the one above that at 16ps. The lower central picture is at 32ps, and so on doubling the time between frames.*

Gaussian like form centred about the line on which the charge event occurred. As would be expected the width of the distribution increases with the distance between the event and the contact.

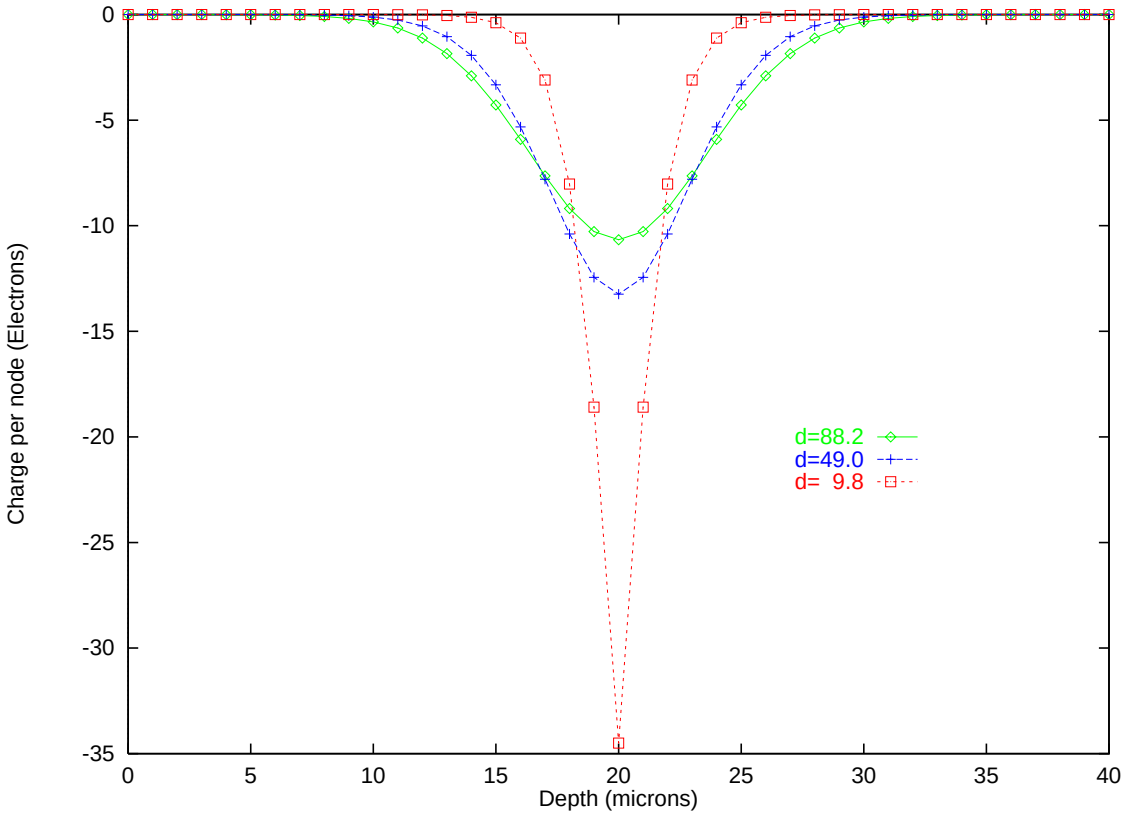

Figure 4: *The charge distribution for the 2D structure with 200 e-h pairs generated at three different depths of 9.8, 49 and 88.2 microns.*

In Figure 5 the log of the charge density is plotted against the square of the distance from the mean. For a pure Gaussian distribution a linear relationship would be expected. The results are close to linear, except in the $d = 9.8$ case. The latter results may well be affected by the coarseness of the mesh for events this close to the contact.

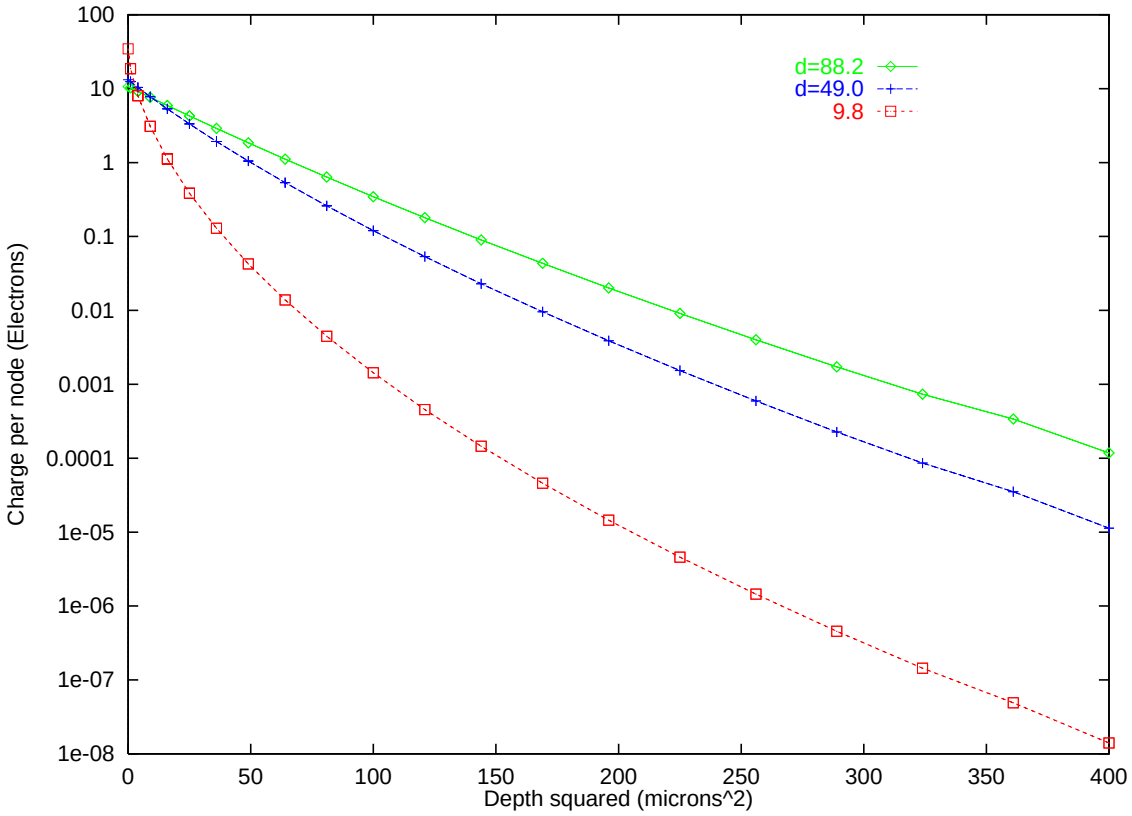

Figure 5: *The charge data of Figure 4 plotted on a log scale as a function of the square distance from the mean. For a Gaussian this should show a linear relationship.*

6 Fitting Gaussian forms to the charge distribution

It will be assumed that a Gaussian is a reasonable representation of the charge distribution. Since the mean of the distribution is known to lie on the centre line (and the results show almost perfect symmetry about this), there are only two parameters available for fitting a Gaussian to the data: the Gaussian width σ and the height of the function. If the data is normalised by dividing by the total charge collected along the plane of interest, then it is only necessary to fit the single parameter σ. This fitting can be done using a least squares approach, for example using the `fmins` function within Matlab [5]. In fact we have retained the mean as a parameter for the fits, but in all cases this is found to be exactly on the centre line.

Since the data points obtained from the simulations are in fact the average of the charge density over the area associated with each contact node, fitting a Gaussian directly to these points can lead to some error, especially when the mesh is relatively coarse. One alternative which avoids this particular source of error is to fit an error function to the partial sums. If q_j is the normalised charge density collected on the j^{th} contact, then $Q_i = \sum_{j=1}^{i} q_j$ is the current collected from $-\infty$ to $x_i + h/2$, where x_i is the position of the contact node and a uniform mesh spacing of h has been used. If a Gaussian is a good representation of the data, the Q_i values should then take the form:

$$Q_i = \frac{1}{\sigma\sqrt{2\pi}} \int_{-\infty}^{x_i+h/2} \exp(-x^2/2\sigma^2)dx = \frac{1 + \mathrm{erf}(x/\sqrt{2}\sigma)}{2} \tag{9}$$

In this case it has been assumed that the origin has been shifted to the mean. This should give a more accurate fit for data that is coarse due to limited resolution of the grid. However, results are still subject to errors due to using a coarse grid.

In Figure 6 three sets of 2D charge distribution data are shown in normalised form along with the Gaussian fits that have been made to them. In this case the Gaussians are fitted directly, rather than using the error function method. In the first two cases the fits appear to be very satisfactory. For the third case, with $d = 9.8\mu m$, the fit is poor. As was seen in Figure 5, this set of data does not show the form expected of a Gaussian, hence it is not surprising that the fit is poor. The resolution of the data on the mesh points is inadequate in this case, as the event is very close to the contact. A simulation with a more refined mesh in this region is needed in this case. To this end a few simulations have been made with about twice the mesh resolution in each direction, the resolution increased partly by using more nodes in the mesh and partly by making the device narrower. These will be compared with the standard mesh results below.

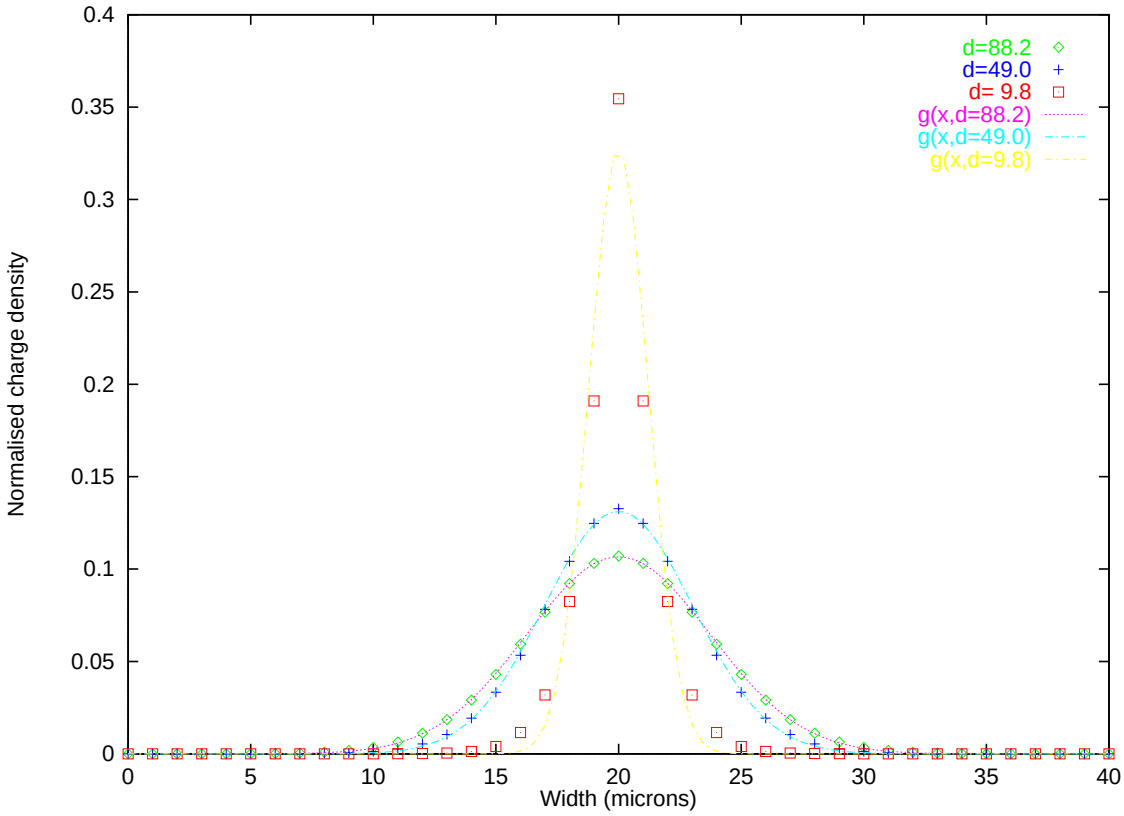

Figure 6: *The normalised charge density data for the three 2D cases along with least squares Gaussian fits.*

7 2D charge spreading results

In Table 1 the measured Gaussian widths of the charge distribution are listed for a range of depths and two different charge densities. A few results are also given for simulations with approximately twice the standard grid resolution.

Charge=200e-h/μm / 3362 node mesh		
Depth (μm)	σ_{gauss} (μm)	σ_{erf} (μm)
9.8	1.127	1.525
24.5	2.180	2.274
39.2	2.746	2.810
49.0	3.016	3.068
63.7	3.332	3.371
73.5	3.505	3.537
88.2	3.727	3.752
Charge=200e-h/μm / 5822 node mesh		
Depth (μm)	σ_{gauss} (μm)	σ_{erf} (μm)
11.76	1.680	1.733
50.96	3.244	3.233
Charge=1000e-h/μm / 3362 node mesh		
Depth (μm)	σ_{gauss} (μm)	σ_{erf} (μm)
24.5	2.67	2.753
39.2	3.466	3.488
49.0	3.822	3.817
63.7	4.214	4.180
73.5	4.421	4.374
Charge=1000e-h/μm / 5822 node mesh		
Depth (μm)	σ_{gauss} (μm)	σ_{erf} (μm)
11.76	2.153	2.186
50.96	4.204	4.042

Table 1: *Fitted Gaussian widths for the 2D data.*

The results from Table 1 are plotted, along with the theoretical approximation σ_t, in Figure 7. In this plot we have used the error function widths. It can be seen that the approximate expression is quite close to the data for the lower initial charge density. Though the results on the standard mesh fall below σ_t at the lowest depths, this maybe due to the coarseness of the mesh. The results on the more refined mesh with the same charge density indicate that the standard mesh results slightly underestimate the true widths.

The results at the higher initial charge density are about 0.5 to 0.8μm wider than those at 200e-h/μm. The width of the spread should increase with charge density due to the two effects of screening of the electric field by the charge and the enhanced lateral spreading due to self repulsion. These effects appear small in the 200e-h/μm case, but significant in the 1000e-h/μm one. In Figure 8 several width results are plotted for different initial charge

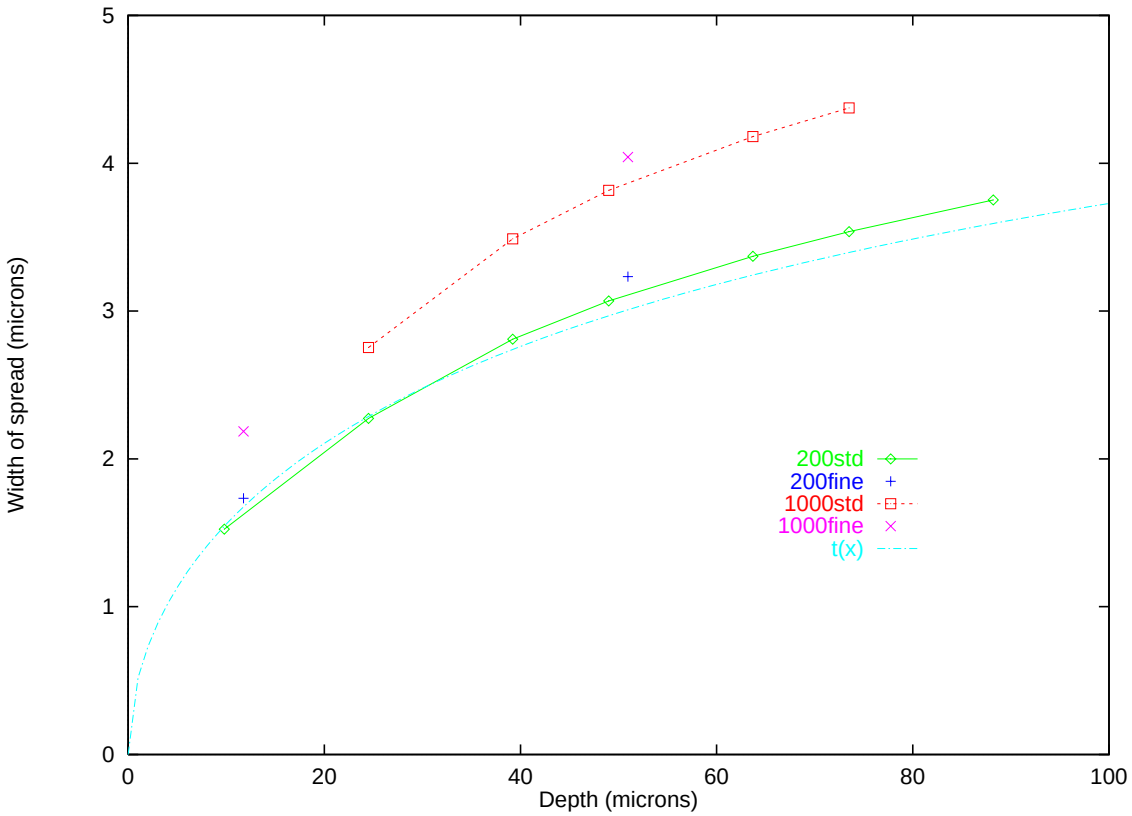

Figure 7: *Charge spreading as a function of depth from the collecting contact. The width shown is the σ obtained from an error function fit to the data. The lower curve is for an initial charge density of 200 e-h/μm and the upper one with 1000 e-h/μm. The $t(x)$ is the theoretical approximation σ_t.*

density events, all at a depth of $d = 49\mu m$. There is a linear relationship between the two quantities up to charge densities of about 1000e-h/μm, with some slight deviation below this by 2000e-h/μm.

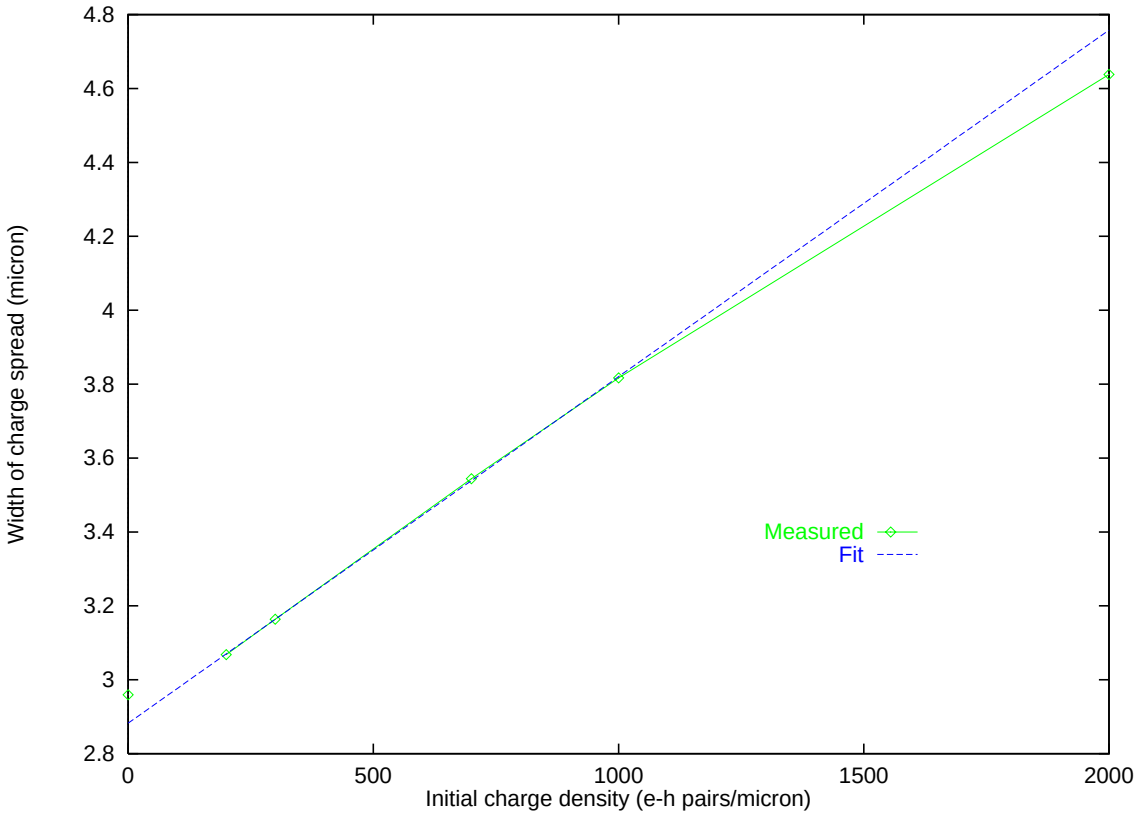

Figure 8: *Charge spreading as a function of initial charge density in 2D. All results are for events at $d = 49\mu m$. A line has been fitted to the first four data points. The data point on the left axis is the theoretical approximation.*

The effect of the mobility on the spreading of charge was seen to cancel out of the expression for σ_t in Equation (8). Simulations using holes rather than electrons have shown the spread to be the same, to within 1%, as when using electrons. Similarly, using the field dependent mobility model only causes very small changes in the measured widths, even though the transit time is quite different.

All the above data refers to transport in a $100\mu m$ device with 40V reverse bias. A few simulations have also been made on a $300\mu m$ structure where the n-region has been extend to $298\mu m$ while keeping all the doping levels the same. This device requires a higher voltage to fully deplete it up to the contact, and a reverse bias of 230V has been used in these simulations. Fitting the electric field of Equation (1) gives $\alpha = 9.80\times10^{-2}V/\mu m$ and $\beta = 4.56\times10^{-3}V/\mu m^2$. Using these values in Equation (8) predicts a width of $\sigma_t(250) = 5.38\mu m$ for an event at a depth of $250\mu m$. Measured widths at this depth are $\sigma = 5.69\mu m$ for 200 e-h/μm and $\sigma = 6.96\mu m$ for 1000 e-h/μm. Linear extrapolation from the two measured results to the zero charge limit gives a value of $\sigma = 5.37$, in good agreement with the predicted σ_t.

8 3D charge spreading results

In Table 2 the Gaussian widths are reported for simulations with 3 different sized charge events at a range of depths. The sizes used are 250, 1000 and 1750 electron hole pairs and in all cases the mesh contains 19404 nodes.

Charge=250e-h		
Depth (μm)	σ_{gauss} (μm)	σ_{erf} (μm)
20.63	1.74	1.67
36.11	2.27	2.31
49.00	2.65	2.69
64.47	2.99	3.02
79.95	3.25	3.27
Charge=1000e-h		
Depth (μm)	σ_{gauss} (μm)	σ_{erf} (μm)
20.63	1.88	1.85
36.11	2.48	2.52
49.00	2.86	2.88
64.47	3.19	3.20
79.95	3.44	3.45
Charge=1750e-h		
Depth (μm)	σ_{gauss} (μm)	σ_{erf} (μm)
20.63	2.02	2.02
36.11	2.68	2.69
49.00	3.04	3.05
64.47	3.36	3.37
79.95	3.61	3.61

Table 2: *Fitted Gaussian widths for the 3D data.*

These results are plotted in Figure 9 using the error function values. Also shown is the approximate expression σ_t. Again the widths are seen to increase with the size to the charge generation event. Going from 2D to 3D there is no clear relationship between the line charge densities of the former and the charge values of the latter. It may be expected that the low charge limits of the 2D and 3D results should be similar.

The results are again close to the approximate expression σ_t, which ignores charge self interaction. The lower charge results lie about 0.2 to 0.5μm below σ_t while the 2D results were mainly above this expression, though the charge density levels used in 2D are not directly comparable with the 3D values. From the trends seen in the 2D results it is expected that a more refined mesh will increase the measured spreading in 3D.

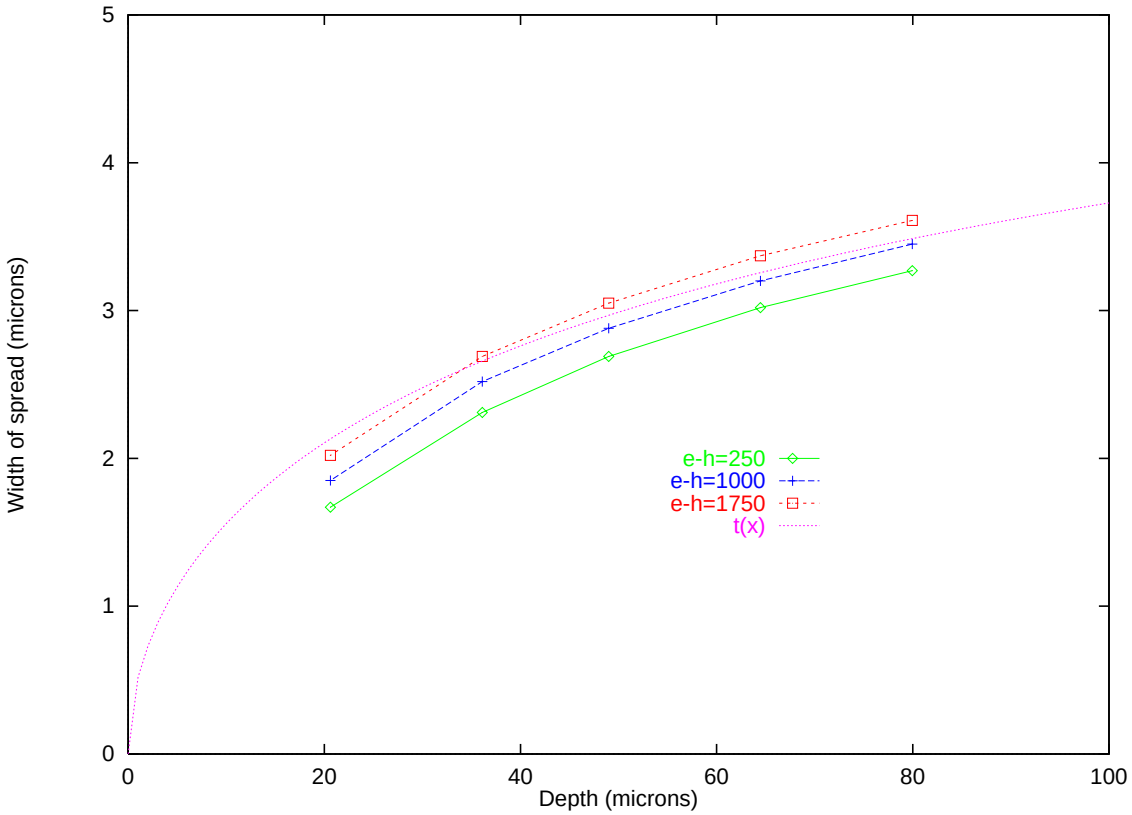

Figure 9: *Charge spreading as a function of depth from the collecting contact. The width shown is the σ obtained from an error function fit to the data. The $t(x)$ is the theoretical approximation σ_t.*

9 Surface for interpolation of 3D data

A goal of the work was to provide a simple way of getting the charge distribution information for any event occurring within the device. The results above show that the spread of charge after an event can be reasonably approximated by Gaussian distributions and that the relationship between event depth and spread at readout modelled by a function of the form of Equation (8) for σ_t.

The exact parameterisation of σ_t has been arrived at by a number of assumptions and approximations to the actual physical processes. As the effect of the charge on the local electric field has been ignored, there is no prediction of the way in which the width of the spread depends upon the amount of charge generated. However the depth/spread trends seem well represented.

To form a depth/spread surface suitable for interpolation, the data from the three 3D tests has been fitted with a function of the same form as Equation (8) save that values of α and β have been used as fitting parameters. This could be viewed as modifying the assumption on the effective electric field due to the presence of the variable dipole field generated by the charge cloud.

Table 3 gives the results of this fitting process and Figure 10 show the resulting surface.

Charge $(e-h/\mu m)$	α $(V/\mu m)$	β $(V/\mu m^2)$
1750	0.2246	0.002469
1000	0.2729	0.001864
250	0.3439	0.000903

Table 3: Table of fitted α and β values

As with the 2D data, the dependence of the spread on the amount of charge is very close to linear over the range of 0 to 1750 electron hole pairs. The gradient of width w.r.t. charge is about $2.4 \times 10^{-4} \mu m$ to $2.7 \times 10^{-4} \mu m$ per electron-hole pair. The extrapolation of the data to zero charge gives widths which lie below the expression σ_t by about $0.3 \mu m$ at the mid point. This compares with an undershoot of less than $0.1 \mu m$ for the zero charge limit in the 2D results at the same depth. Due to the increase of width with mesh refinement that was observed in the 2D results, and the fact that the 3D mesh provides lower resolution than either of the 2D meshes, it is not unreasonable to expect that the 3D data may underestimate the true widths.

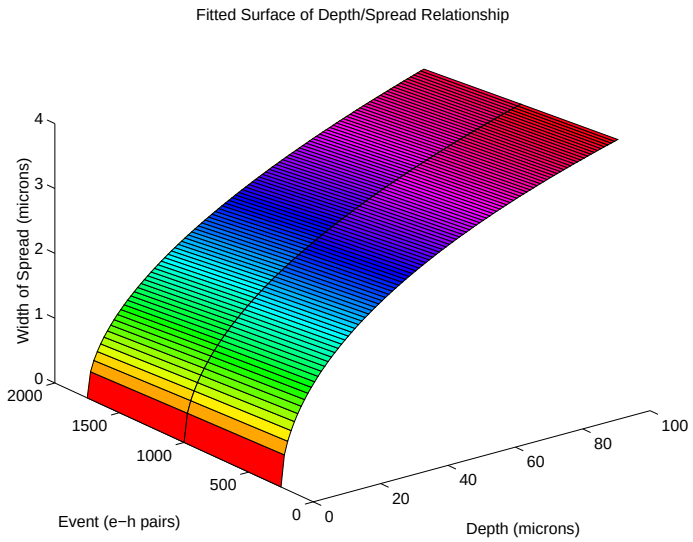

Figure 10: Surface of *depth* verses *spread*

10 Conclusions

The spreading of charge from a point generation event up to the time it is collected at a contact has been simulated in two and three dimensional fully depleted diodes. These measurements have mainly been made on devices with a drift length of $100\mu m$ and a doping of $3 \times 10^{12} cm^{-3}$. However the parameters α and β used in Equation (8) can easily be determined for other uniform doping levels and size of depletion region. In conditions similar to those studied in this report it is expected that the above equation can be used as a reasonable approximation to the low charge limit of the spreading. A linear increase of spread with the amount of charge is predicted by our present results, and only a few simulations should be required to fully determine the spread for the size of charge generation events likely to arise from X-ray strikes.

While it is possible to fit a surface to the simulation data, as shown in section 9, the present 3D results are subject to some uncertainty due to the coarseness of the mesh used. For many purposes it maybe sufficiently accurate to use the expression for σ_t and combine this with the measured gradient of width with respect to charge event size, obtained from two simulations at a typical depth.

11 Acknowledgements

The authors wish to thank Andrew Holland for many helpful discussions about these simulations and the IMPACT project which funded this work.

References

[1] *MCNP - A Generalised Monte Carlo N-Particle Transport Code - Version 4B*, J.F.Briemeister (ed), LA-12625 March 1997.

[2] *Modifications of the EVEREST Device Modelling Software to Simulate Charge Generation Events*, R.F.Fowler, J.V.Ashby and C.Greenough, RAL Report, to be published.

[3] *Three dimensional algorithms for a robust and efficient semiconductor simulator with parameter extraction: the EVEREST final report*, C.Greenough, Report RAL92082, Rutherford Appleton Laboratory, Chilton, 1992.

[4] *EVEREST Pre-processor user manual Version 3.0*, N.Ferguson *et al*, Report RLUR17908, Rutherford Appleton Laboratory, Chilton, 1990.

[5] *MATLAB version 4 user's guide* The Mathworks Inc., Prentice-Hall (1995).

[6] *Mathematical Methods for the Physical Sciences*, K.F.Riley, Cambridge University Press, 1974, page 252.

[7] *IMPACT - Innovative Microelectronic Pixellated sensors and Advanced CCD Technology*, UK Technology Foresight Challenge Proposal, March 1996.